Forest Ecology and Management 552 (2024) 121585

Contents lists available at ScienceDirect

Forest Ecology and Management

journal homepage: www.elsevier.com/locate/foreco

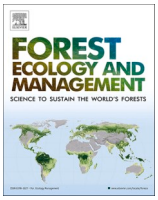

Self-thinning of Scots pine across Europe changes with solar radiation, precipitation and temperature but does not show trends in time

Astor Toraño Caicoya [a,b,*], Peter Biber [a], Miren del Río [c], Ricardo Ruiz-Peinado [c], Catia Arcangeli [d], Robert Matthews [d], Hans Pretzsch [a]

[a] TUM School of Live Sciences, Chair of Forest Growth and Yield Science, Hans-Carl-von-Carlowitz 2, Freising D-85354, Germany
[b] Technical University of Munich, Germany, Hans-Carl-von-Carlowitz 2, Freising D-85354, Germany
[c] INIA-CSIC, Forest Research Centre, Madrid, Spain
[d] Forest Research, Alice Holt Lodge, Farnham, Surrey, United Kingdom

ARTICLE INFO

Keywords:
Silviculture
Maximum density
Carrying capacity
Forest modelling
Biomass
Mortality
Site quality
Climatic change

ABSTRACT

The effects of site and climate on the self-thinning line, a key characteristic that defines forest dynamics, have been the subject of research for decades. However, contrasting results have generally been found. To adapt management practices for widely distributed species, especially considering the impact of climate change, it is crucial to understand the variables and their effects on the self-thinning line. We conducted a systematic analysis based on 77 trial plots from 62 long-term experiments across Europe, covering the distribution range of Scots pine. Our focus was on unthinned conditions since 1975. Using a linear mixed model, we examined the effects of each statistically significant variable, separating the influences on the slope and the intercept. Our observations revealed that parameters enhancing species tolerance, such as shortwave solar radiation, flatten the slope of the self-thinning line. Conversely, temperature and precipitation, which reduce self-tolerance and increase intra-specific competition, lead to an increase in the slope. Balancing the effects between these aspects results in a maximum negative slope at mid-latitudes. In terms of the intercept, we found compensating effects among the analyzed factors, indicating a monotonic increase with decreasing latitude and increasing radiation. Although there were no significant changes in the self-thinning line since the 1990 s, we observed an increase in mortality, suggesting an accelerated self-thinning process. Site and climatic differences across the distribution range of Scots pine influenced the self-thinning line, whereas no trends with time could be observed. Therefore, management strategies and models based on self-thinning need to be adapted to different latitudes. While climate changes have not yet impacted the trajectory significantly, a continuous rise in temperature, coupled with high precipitation, may accelerate self-thinning and result in increased biomass accumulation.

1. Introduction

The principle of self-thinning is widely recognized as one of the most well-documented examples of natural selection (Zeide, 2010). It describes the exponential decline in tree numbers as age or mean size increases, primarily due to natural mortality (Lonsdale and Watkinson, 1982). This concept is crucial for understanding stand dynamics and potential productivity (Jack and Long, 1996) and holds significant importance in both forestry and ecology (Condés et al., 2017; Lonsdale and Watkinson, 1982). Given the uncertain future of climate change, gaining a better understanding of the climate's influence on self-thinning is essential. It will enhance our ability to manage and model forest ecosystems and enable us to determine forests' carrying capacity more accurately, thereby improving the design of silvicultural guidelines (Rodríguez de Prado et al., 2020). This understanding will help us avoid overly dense and unstable stands, allowing us to maximize sustainable harvests. Additionally, changes in the self-thinning line will influence biomass accumulation patterns and mortality rates, thereby impacting carbon storage in forests.

Tree growth exhibits a geometric progression until it is constrained by the onset of senescence. However, due to the inherent limitations of environmental resources, the sustained exponential increase in individual tree numbers is unsustainable. Eventually, a threshold or maximum capacity is reached or closely approached (Harper, 1977).

* Corresponding author at: TUM School of Live Sciences, Chair of Forest Growth and Yield Science, Hans-Carl-von-Carlowitz 2, Freising D-85354, Germany.
E-mail address: astor.torano-caicoya@tum.de (A. Toraño Caicoya).

https://doi.org/10.1016/j.foreco.2023.121585
Received 3 August 2023; Received in revised form 23 October 2023; Accepted 13 November 2023
Available online 24 November 2023

The precise mechanisms and spatial dynamics underlying this threshold are contingent upon species-specific patterns of space occupancy and the associated site-specific factors that shape them.

Plant populations have repeatedly been found to approach and then follow a dynamic thinning line. For many years, all such lines were widely perceived as having a slope of roughly –3/2 (Begon et al., 2006). In forestry the self-thinning of forest stands is usually expressed as the relationship between stand density *N* and the quadratic mean diameter *dq*. Reineke (1933) found that this relationship can be expressed using Eq. 1:

$$\ln(N) = a + b \bullet \ln(dq) \quad (1)$$

The slope b of the self-thinning line, or maximum size-density relationship is often assumed to be independent of species (according to Reineke, b = –1.605). However, this assumption has been put into question recurrently in forestry literature leading to contrasting explanations (Condés et al., 2017) and many authors (von Gadow, 1986; Weiskittel et al., 2009; Zeide, 2010; Zhang et al., 2018) have discussed the meaning and values of the intercept and slope of the self-thinning line.

Pretzsch and Biber (2005) found that the slope of the self-thinning line varies among different European forestry species, ranging from –1.789 to –1.424. This shows that the relationship between tree density and size differs depending on the species. Regional variations in the self-thinning line can be influenced by genetic and environmental factors. The allocation of resources to standing biomass, which is affected by maximum stand density, can also vary across latitudes. Furthermore, it's important to consider that variations in data types and parameter estimation techniques can introduce additional uncertainties in the analysis (Forrester et al., 2021; Peters et al., 2018). Studies based on permanent plot data have shown that stands self-thin at different levels of maximum density. Several investigations, from national (Aguirre et al., 2018; Charru et al., 2012) to large-scale (Condés et al., 2017) studies using inventory data, have explored this question further. Some studies have shown that species specific shade tolerance has an impact on maximum density and self-thinning (Bose et al., 2018; Ducey et al., 2010). However, there is still a lack of consensus regarding the underlying processes driving the observed variation (Reynolds and Ford, 2005). Therefore, a relevant question remains: which specific resources influence the relationships within the stand and modify the self-thinning line (Rodríguez de Prado et al., 2020)?

In environments with limited light availability, self-thinning occurs as a result of crown adaptation to intercept radiation (Harper, 1977; Peters et al., 2018; Zeide, 2010). Crown architecture plays a crucial role in controlling self-thinning processes in such light-limited environments. Changes in nutrient or water availability can influence the rate of self-thinning without altering its overall trajectory. For instance, Pretzsch and Biber (2021) observed the effect of nitrogen (N) availability in the soil on self-thinning dynamics. In contrast, self-thinning in dry environments displays different characteristics. For example, in ecosystems like Savannas, where water availability rather than radiation/light is the limiting factor, trees are spaced widely (Belay and Moe, 2012). The dynamics of self-thinning in these dry environments are shaped primarily by the availability of water resources. Overall, the interplay between light, nutrient availability, water resources, and crown architecture determines the specific patterns and mechanisms of self-thinning in different environmental conditions.

While solar radiation tends to remain relatively stable, precipitation and temperature can undergo changes over time, particularly under the influence of climate change (Pretzsch et al., 2017). In the 1980s, concerns about air pollution and climate change leading to widespread ecosystem collapse were prominent in public discussions. During this period, scientific studies began to report accelerated forest growth in Central Europe (Pretzsch et al., 2014). However, despite the clear trend observed in many regions of Central Europe, our understanding of the long-term implications for stand dynamics and forest management remains limited (Gadow, 2006; Woodall and Weiskittel, 2021).

In this study, we employed a distinctive compilation of data from permanent plots of Scots pine (*Pinus sylvestris* L.) across Europe. This dataset comprises a diverse array of climatic and site conditions, making it particularly valuable as Scots pine is not only one of the most significant commercial tree species but also widely distributed across the region. These long-term forest experiments offer a valuable record of stands with well-documented histories, encompassing details on establishment, silvicultural treatments, and disturbances. They offer time series data on stand development, making them suitable for biomonitoring in both managed and unmanaged forests, as well as for modeling purposes (Peters et al., 2018; Pretzsch et al., 2019).

Our hypothesis is that the intercept and slope of the self-thinning line vary with environmental conditions (Pretzsch and Biber, 2005). Understanding how these conditions affect the self-thinning patterns, and whether they modify the slope, intercept, or both, has important implications for silviculture, biology, and climate research (del Río et al., 2001).

The primary objective of this study is to model the self-thinning process, with a focus on providing new insights into the effects of site and climate on self-thinning patterns, as well as understanding their physiological responses and implications. Rather than aiming for precise modeling, our main goal is to offer a general overview and address the following research questions:

Q1: Do the slope and/or the intercept of self-thinning line depend on site factors?

Q2: Which are these factors, and how do they influence the self-thinning line?

Q3: Can climate change affect components of growth?

2. Materials and methods

2.1. European long-term research plots

We used a compilation of long-term research plots of Scots pine from various locations across Europe (Pretzsch et al., 2019). These plots encompass a wide range of latitudes (over 20°) and represent three distinct biomes: boreal, temperate, and Mediterranean. We specifically selected monospecific even-aged stands that were either unthinned or had minimal thinning, with only the removal of dead or dying trees. This selection was made to ensure that the stands were likely to exhibit self-thinning and full canopy closure (Reynolds and Ford, 2005). To further ensure that the stands in our analysis truly exhibited self-thinning, we excluded data from years that showed a positive slope in the log-log relationship and ensured a mortality rate >1 %. By focusing solely on this part of the self-thinning line, we aim to simplify the self-thinning model and avoid unnecessary complexities.

In total 77 plots from 62 different experiments were available for the selected conditions. The geographical distribution of the plots can be seen in Fig. 1 and the site characteristics are summarized in Table 1.

The plot size varies from 0.15 to 0.5 ha. The most relevant available variables for this study were: stand density per hectare (*N*), quadratic mean diameter (*dq*), age and inventory year. Additionally, we calculated the local *SDI*, by fitting the exponent of the Reineke expression locally (for each trials' *N* and *dq*), and mortality rate, and biomass were used as growth components, to study changes in time (Table 2). Biomass was calculated based on the equations developed by Forrester et al. (2017). A detailed description can be found in the Supplementary material (S1: Conversion of wood volume to biomass).

2.2. Site and climate variables

We obtained climate and site parameters by extracting data from two primary sources. The first source was the Gridded Agro-Meteorological Data from the European Commission Joint Research Center (JRC), which provided data with a 25 × 25 km resolution grid covering the

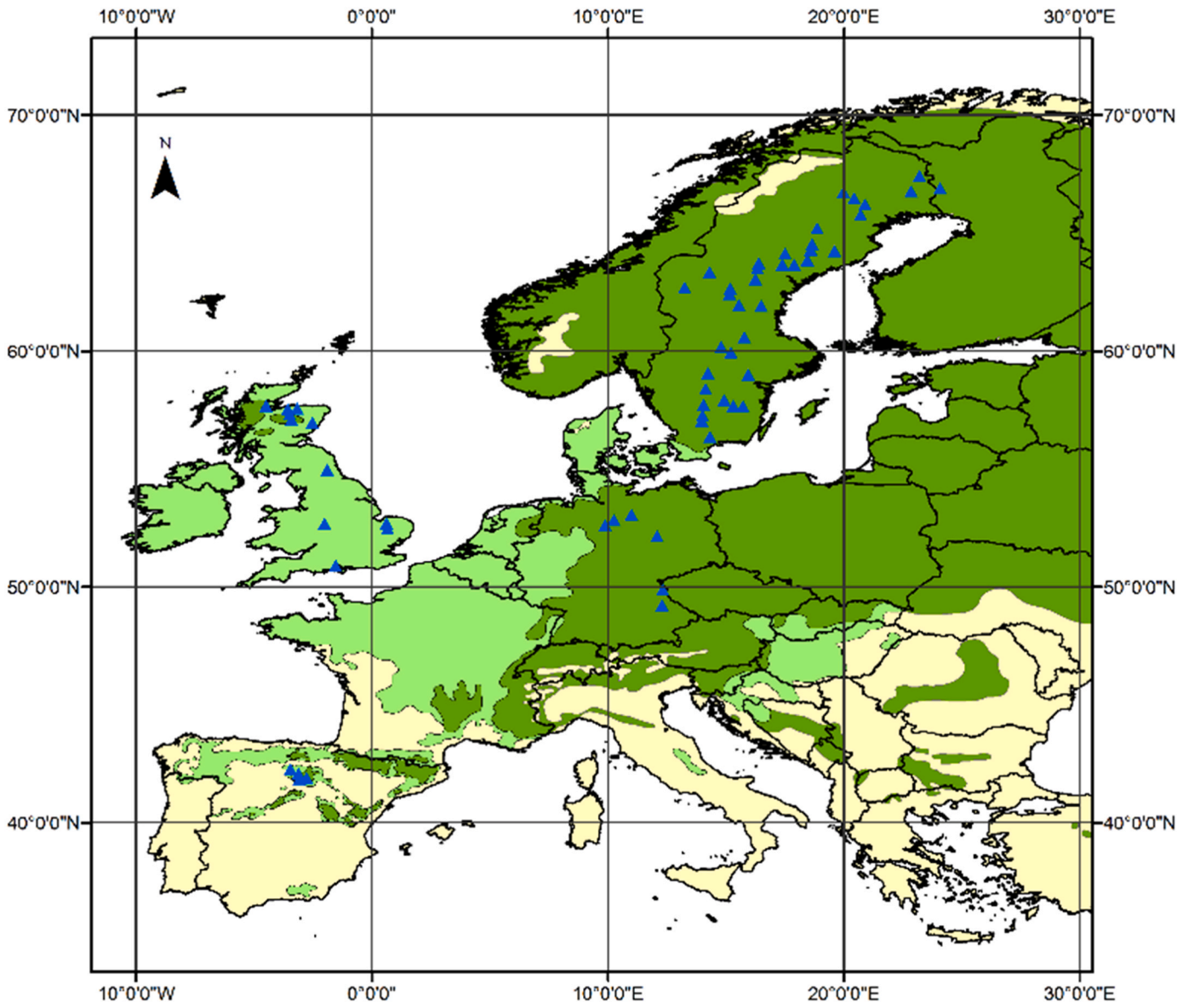

Fig. 1. Location of the research experiments across Europe (blue triangles) over the natural (dark green) and actual (light green) distribution of the Scots pine in Europe.

years 1975–2014 (CGMS, 2014). From this dataset, we extracted the yearly mean temperature (*Temp* in °C), total annual precipitation (*Prep* in mm), and calculated the annual length of the vegetation period (*LenVp* in days), defined as the number of days with an average temperature above 10 °C. The second source of data was the Inter-Sectoral Impact Model Intercomparison Project (ISIMP, 2022). We retrieved the daily intervals of solar radiation (short wavelength) (*ShortRad* in W m-2) from this dataset and calculated the mean solar radiation per site and year. Additionally, we estimated the Martonne aridity index (*M*) (Martonne, 1926) using the following expression:

$$M = Prep/(Temp + 10) \tag{2}$$

2.3. Model building

We conducted our analysis by selecting site and climate variables with low correlation (see Supplementary Material Fig. S1). We addressed our first two research questions (Q1-Q2) using a mixed linear regression model based on Reineke's logarithmic form of the self-thinning line (Eq. 1). Reineke derived from it his stand density index SDI which is, at a given N and dq, the number of trees per unit area at a reference diameter of 25 cm (~10 in.):

$$SDI = N \bullet (dq/25)^{b}, \tag{3}$$

$$\ln(SDI) = \ln(N) + b \bullet \ln(dq/25). \tag{4}$$

If we, in turn put ln(N) on the left side of the equation:

$$\ln(N) = \ln(SDI) - b \bullet \ln(dq/25), \tag{5}$$

or in more compact notation with $\ln(SDI) = a$:

$$\ln(N) = a - b \bullet \ln(dq/25), \tag{6}$$

we have a model which estimates the (*ln*) stem number for a given *dq*, but where the intercept is the *ln (SDI)*. This has no influence on the slope; however, the intercept is automatically an *SDI*. This is very convenient, since the *SDI* is descriptive, it is a number that forest scientists and practitioners are used to working with and allows a very straightforward and easy interpretation of the intercept. With this transformation, we defined a general linear mixed model that included

Table 1
Overview of the main site structural characteristics. dq stands for quadratic mean diameter, N for the number of trees per hectare, H100 the dominant height at age 100 and SDI the Stand Density Index.

Country	Age [years]			year		dq [cm]			N [trees ha^{-1}]			H100 [m]			SDI [ha^{-1}]			Total Biomass [Mg ha^{-1}]			Mortality rate [% year^{-1}]		
	min	mean	max	min	max	min	mean	max	min	mean	max	min	mean	max	min	mean	max	min	mean	max	min	mean	max
Utd. Kingdom	44	74	136	1975	2008	14.66	26.6	51.65	334	1231	3108	15.4	22.8	32.7	668	1133	1836	140	314	615	0.000	0.014	0.041
Germany	16	54	122	1976	2010	6.8	16.3	31.8	348	1969	5313	6.5	17.3	25.7	400	1040	1746	8.0	132	290	0.000	0.010	0.066
Spain	22	61	90	1982	2008	13.0	20.0	26.3	1142	1677	2680	8.3	16.5	25.2	893	1319	1843	40	210	431	0.000	0.012	0.043
Sweden	31	57	86	1975	2009	10.87	15.9	24.75	676	1681	2920	10.5	17.8	24.0	640	1030	1481	42	135	269	0.000	0.011	0.048

Table 2
Overview of the main site geographic and climatic characteristics. Temp stands for mean annual temperature, Prep the total annual precipitation, ShortRad the mean short wavelength radiation per year and LenVp the length of the vegetation period.

Country	Temp [°C]			Prep [mm]			ShortRad [W m^{-2}]			LenVp [days]			Latitude [°]			Elevation [m asl]			Martone Index		
	min	mean	max	min	mean	max	min	mean	max	min	mean	max	min	mean	max	min	mean	max	min	mean	max
Utd. Kingdom	5.1	8.7	11.2	473.8	711.8	1093.2	87.9	106.2	140.8	64	154	217	50.9	55.0	57.7	26	108	468	25.5	38.0	55.0
Germany	7.1	8.9	10.9	378.3	631.3	989.7	104.0	119.0	132.9	143	174	206	49.2	51.0	53.1	29	262	529	19.0	33.4	51.4
Spain	9.3	10.8	12.8	369.8	569.7	840.8	160.2	171.4	193.1	161	187	245	41.9	42.0	42.3	961	1080	1155	17.9	27.5	41.3
Sweden	–1.9	2.6	8.0	261.4	470.0	1407.0	93.3	106.9	126.8	48	103	161	56.4	62.5	67.4	43	222	642	17.3	37.7	86.8

all the site and climatic selected variables and all possible two-way interactions among them in a combined intercept (a), which is in fact the *SDI*, and in the slope (b), resulting in the following expression:

$$\ln(N_{ijk}) = a_0 + a_1 \bullet Temp_{ijk} + a_2 \bullet Prep_{ijk} + a_3 \bullet ShortRad_{ijk} + a_4 \bullet LenVP_{ij} + \left(ln(dq_{ijk}/25) + c_{ij}\right) \bullet \left(b_0 + b_1 \bullet Temp_{ijk} + b_2 \bullet Prep_{ijk} + b_3 \bullet ShortRad_{ijk} + b_4 \bullet LenVP_{ijk}\right) + c_i + c_{ij} + c_{m(ijk)} + \varepsilon_{ijk} \quad (7)$$

where indexes *i*, *j* and *k* represent the nested data levels trial, plot, and survey. An additional random effect is $c_m(ijk)$ which indicates the year in which the *kth* survey of plot *j* in trial *i* was conducted. To evaluate the possible effect of clustering by genetic adaptations was assessed by adding a random effect term on the slope on plot and trial level c_{ij}.

Next, we performed an automated model selection procedure using the 'dredge' function from the R package MuMIn (Barton, 2020) to identify the sub-model with the best combination of independent variables, and additionally evaluating the resulting combinations for physiological plausibility. In this procedure, if a variable (n) is found to be significant, it indicates that the corresponding site variable has an influence on the Stand Density Index (*SDI*), which represents the intercept. Similarly, if the slope parameter (b_n) is found to be significant, it suggests that a site variable (n) influences the slope of the self-thinning line.

Since the Martone Index is highly correlated with the precipitation (Supplementary material, Fig. S1), we decided to test it independently. In this way, similarly to Paterson's vegetation productivity index, especially in humid sites, it can be interpreted as an indication of site quality and the temporal variation of productivity and forest growth (Pretzsch et al., 2023).

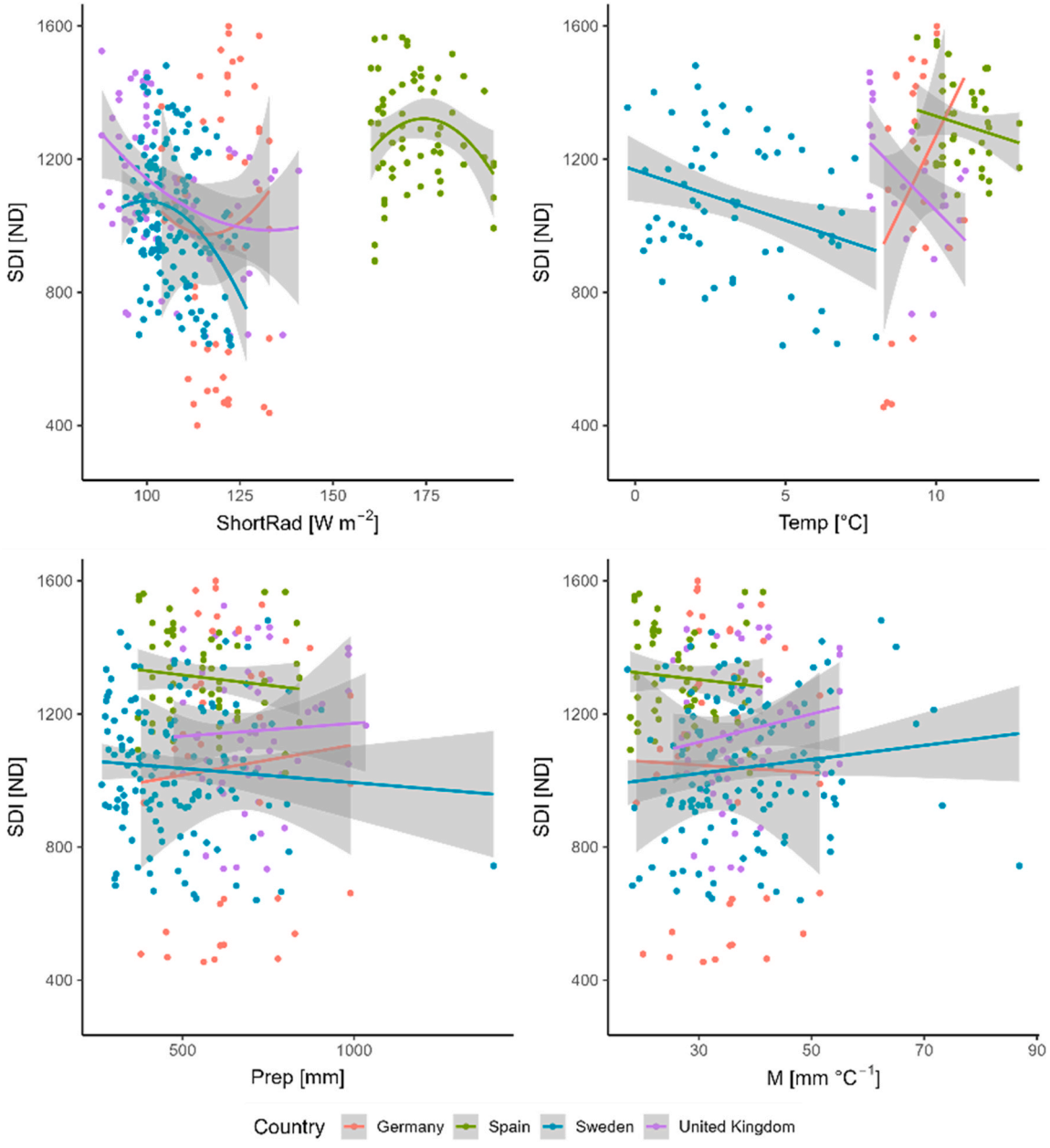

Fig. 2. Site variables against the Stand Density Index (SDI) represented per single plot and inventory in time. The curves are the result of linear fit model (y = a+bx) for each trial plot with the standard error represented by the grey bands. The SDI was estimated locally for each trial fitting the exponent of the Reineke's expression in each trial based on the local N and dq. Note that grouping by country is just for display and does not represent the self-thinning models.

2.4. Changes with time and growth components

Climate is a dynamic factor that undergoes changes over time, and studies such as Pretzsch et al. (2014) have shown the impact of climate change on forest growth. Specifically, the increase in annual temperature, leading to a longer vegetation period, has been identified as a driver of accelerated growth, especially in those sites where water is not a limiting factor. In this study, we selected the year 1990 as an arbitrary threshold, coinciding with the significant temperature rise of 0.5 °C reported in the first IPCC report (IPCC and WMO, 1992), to assess changes in growth over time.

To further investigate changes in growth patterns, we selected two specific growth components, the rate of mortality and the biomass development, and we tested two simple linear mixed models with the following expression:

$$\ln(Var_{ijk}) = a_0 + a_1 \bullet \ln(age_{ij}) + a_3 \bullet LATITUDE_{ij} + a_4 \bullet \ln(age_{ij}) \bullet LATITUDE_{ij} + c_i + c_{ij} + \varepsilon_{ij} \quad (8)$$

where *Var* stands for the growth component tested.

3. Results

3.1. Climate variables as predictors of changes in the self-thinning line

Fig. 2 provides a visual representation of the relationship between the observed Stand Density Indices (SDIs) and the key site variables relevant to answering Q1 and Q2. As a first exploratory analysis we decided to group and display the sites by countries (instead of grouping them by site and trial as described by the random effects in Eqs. 7 and 8), to display patterns that may include not only site influences but also data collection artifacts. The graph highlights several noteworthy observations. Firstly, the mean annual temperature (*Temp*) exhibits a continuous gradient across the different countries, with Sweden displaying the widest range. Secondly, there is considerable overlap among countries in terms of total precipitation (*Prep*). Lastly, short-wave solar radiation (*ShortRad*) serves as a distinguishing factor, clearly separating the plots in Spain from those in other countries. This differentiation is primarily influenced by factors such as latitude, orientation, and altitude, and remains consistent over time within the scope of this study. Notably, the stands in Spain stand out with the highest mean solar radiation among the countries analyzed.

The relationship between the number of trees per hectare (*N*) and the diameter at breast height (*dq* in cm) in logarithmic scale provides insights into the arrangement of self-thinning lines across the continent (Fig. 3). The graph reveals distinct zonation among the countries, indicating a potential pattern. Specifically, the lines of the Spanish plots tend to be positioned on the higher end of the spectrum, while those of the Swedish plots tend to be on the lower end. This variation suggests differences in the density of trees and their corresponding slopes, highlighting potential regional trends in self-thinning dynamics.

We also examined the significance of the length of the vegetation period a robust indicator of growth changes (Fig. 4) using an ANOVA test, to validate its use as a reference for evaluating alterations in the self-thinning line. The length of the vegetation period significantly increased before and after 1990.

3.2. Self-thinning models

The optimized statistical model based on Eq. 7 revealed that most covariates are statistically significant, except for temperature (*Temp*) in the intercept term. Notably, precipitation (*Prep*), solar radiation (*ShortRad*), and the length of the vegetation period (*LenVp*) exhibit significance, along with the interactions Prep*ShortRad and LenVp*-Temp. In terms of the slope term, *ShortRad*, *Temp*, and *Prep* were statistically significant.

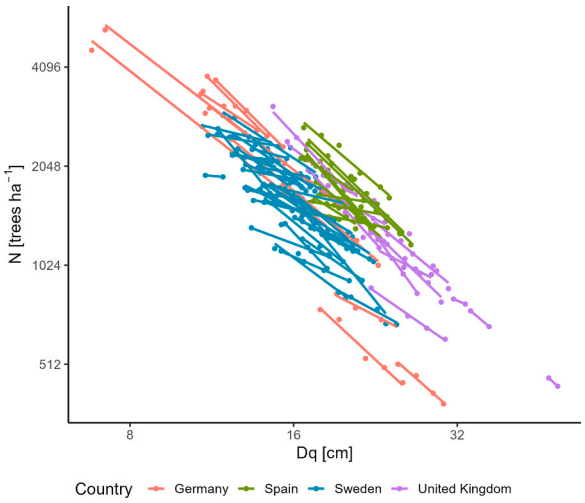

Fig. 3. Number of trees per hectare (N) plotted against quadratic mean diameter (dq). The lines are the result of linear fit model (ln(y)=a+b*ln(x)) for the each trial plot. Note that grouping by country is just for display and does not represent the self-thinning models.

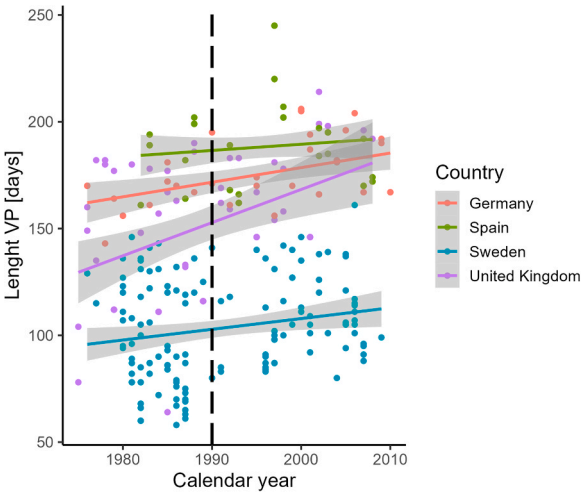

Fig. 4. Length of the vegetation period (LenVp) against the calendar year for the sites anylized in this study. The lines are the result of linear fit model (y = a+bx) for the each trial plot. Note that grouping by country is just for display and does not represent the self-thinning models.

To address the high correlation between *Temp* and *LenVp*, and considering the lack of significance for *Temp* in the intercept term, *Temp* was excluded from the model. However, the interaction *LenVp*Temp* was retained as it does not introduce non-linear effects. The resulting selected model, presented in Eq. 9, incorporates these adjustments.

$$\ln(N_{ijk}) = a_0 + a_1 \bullet Prep_{ijk} + a_2 \bullet ShortRad_{ijk} + a_3 \bullet LenVP_{ijk} + a_4 \bullet LenVP_{ijk}Temp_{ijk} + a_5 \bullet ShortRad_{ijk} \bullet Prep_{ijk} + ln\left(\frac{dq_{ijk}}{25}\right) \bullet (b_0 + b_1 \bullet ShortRad_{ijk} + b_2 \bullet Prep_{ijk} + b_3 \bullet Temp_{ijk}) + c_i + c_{ij} + c_{m(ijk)} + \varepsilon_{ijk} \quad (9)$$

The test for the random effect on the slope resulted significant with a decreased AIC (Akaike, 1974). However, the change was minor and did not impact the results. For this reason, we decided to select the simpler model with only random effects on the intercept. This model is easier to interpret and more reproducible (Barr et al., 2013).

Table 3 summarizes the parameter estimates and their significance.

Table 3
Results of fitting Eqn 9 to the permanent plots data. Significance codes '*','**' and '***' indicate P < 0.05, 0.01 and 0.001, respectively. Temp stands for mean annual temperature [°C], Prep the total annual precipitation [mm], ShortRad the mean short wavelength radiation per year [w m^{-2}].

Variable	Parameter	Estimate	P-value	Standard error
Intercept	a_0	6.63	$<2.00 \times 10^{-16}$ ***	1.54×10^{-1}
Prep	a_1	4.17×10^{-4}	6.77×10^{-3} **	1.53×10^{-4}
LenVP	a_2	-1.38×10^{-3}	1.89×10^{-2} *	5.82×10^{-4}
Short Rad	a_3	2.95×10^{-3}	1.01×10^{-2} **	1.14×10^{-3}
Prep x ShortRad	a_4	-3.54×10^{-6}	1.03×10^{-3} **	1.12×10^{-6}
Temp x LenVP	a_5	9.39×10^{-5}	1.26×10^{-3} **	3.73×10^{-5}
log(dq/25)	b_0	−1.43	1.75×10^{-14} ***	1.76×10^{-1}
shortRad x (log (dq/25)	b_1	3.88×10^{-3}	6.68×10^{-3} **	1.42×10^{-3}
Prep x (log(dq/25)	b_2	-2.93×10^{-4}	3.25×10^{-2} *	1.36×10^{-4}
Temp x (log(dq/25)	b_3	-2.57×10^{-2}	3.08×10^{-3} **	8.60×10^{-3}

The effects on the intercept term vary among the variables. The single variables *Prep* and *ShortRad*, as well as the interaction *LenVp***Temp*, increase the intercept, while the single indicator *LenVp* and the interaction *Prep***ShortRad* decrease it. As for the slope, *ShortRad* reduces (flattens) the negative slope, whereas *Prep* and *Temp* increase it (steepen it) (Q2). Residual analyses and QQ plots are depicted in the Supplementary material (Figs. S2–4).

Finally, the model with the Martonne index (*M*) resulted in:

$$\ln(N_{ijk}) = a_0 + a_1 \bullet M_{ijk} + a_2 \bullet ShortRad_{ijk} + ln\left(\frac{dq_{ijk}}{25}\right) \bullet (b_0 + b_1 \bullet M_{ijk} + b_2 \bullet ShortRad_{ijk}) + c_i + c_{ij} + c_{m(ijk)} + \varepsilon_{ijk} \quad (10)$$

The statistical analysis revealed that the Martonne index (*M*) was statistically significant for both the intercept and slope terms, indicating its influence on the self-thinning model. On the other hand, *ShortRad* showed slight significance for the intercept but was non-significant for the slope term (Table 4). Like the previous model, *ShortRad* had positive coefficients for both terms, suggesting that it flattened the slope and increased the intercept.

To further illustrate the tendencies identified in this study, we plotted the estimated self-thinning lines for different latitudes based on the real combinations of site variables from the data (Fig. 5). The

Table 4
Results of fitting Eq. (10) to the permanent plots data Significance codes ".", '*','**' and '***' indicate P ~0.05, < 0.05, 0.01 and 0.001, respectively. ShortRad the mean short wavelength radiation per year [w m^{-2}] and M the Martonne Index [ND].

Variable	Parameter	Estimate	P-value	Standard error
Intercept	a_0	6.59	$<2.00 \times 10^{-16}$ ***	1.61×10^{-1}
M	a_1	6.34×10^{-3}	0.030 *	2.90×10^{-3}
ShortRad	a_2	2.35×10^{-3}	0.061.	1.25×10^{-3}
M x ShortRad	a_3	-5.72×10^{-5}	0.011 *	2.21×10^{-5}
log(dq/25)	b_0	-9.89×10^{-1}	$<2.00 \times 10^{-16}$ ***	1.90×10^{-1}
M x (log(dq/25)	b_1	-7.61×10^{-4}	0.022 *	2.33×10^{-3}
ShortRad x (log (dq/25)	b_2	-5.38×10^{-3}	0.560	1.30×10^{-3}

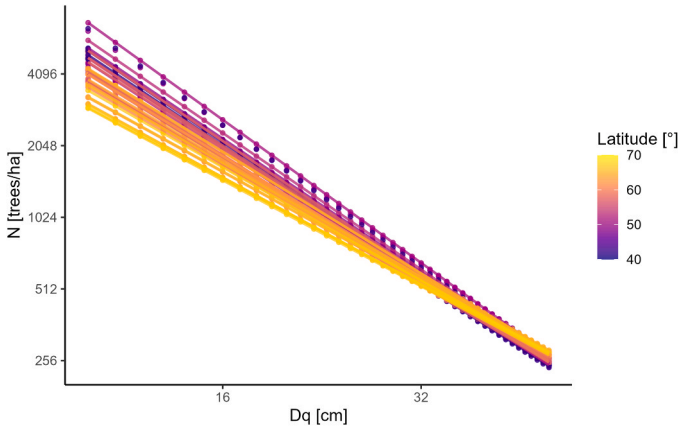

Fig. 5. Self-thinning lines obtained applying the full model Eq. 5 to the real combinations of climate variables for a range of latitudes covering the range from south to north.

observations showed that while *ShortRad* flattened the slope, the positive effect of higher mean temperature in southern latitudes partially compensated for this effect (as indicated by the positive estimates for *ShortRad* and Temp in Table 3). Additionally, *ShortRad* increased the intercept, which was further reinforced by the positive interaction between *LenVp* and *Temp* in Eq. 9. The effect of *Prep* on the self-thinning line was also observed, as it steepened the slope while simultaneously increasing the intercept (Table 3).

In Fig. 5, the self-thinning lines for German and English sites (~52°–54°), characterized by average values for the variables (Table 2), appeared on the upper side of the spectrum. Conversely, the most northern latitudes exhibited the lowest intercepts but also had relatively flat slopes, despite the low solar radiation.

The selected model yielded a range of slopes from –1.469 to –1.049 and intercepts ranging from 6.839 to 6.957 (SDI ~ 900). Fig. 6 displays the intercepts and slopes obtained from the self-thinning lines depicted in Fig. 5. Notably, there is a discernible tendency for the slopes to follow a parabolic curve in relation to latitude. Conversely, the intercepts exhibit a relatively linear trend, decreasing as latitude increases.

To ensure the robustness of the predictors' signs, an additional simplification was tested and can be found in the Supplementary material (Eq. S6, Table S2). This analysis provides further evidence supporting the consistency of the predictors' influence on the self-thinning model.

3.3. Changes in the self-thinning line with time

The length of the vegetation period increased steadily since 1990 for all countries, but in different degree (Fig. 4). The United Kingdom exhibited steeper trends compared to Spain, where the patterns were relatively flatter. The change in length of the vegetation period was statistically significant after the 1990s

After applying the model (Eq. 9) to the data before and after 1990, we found that the change in the self-thinning line was not statistically significant (Q3). Fig. 7 illustrates how the line remains nearly constant after 1990, and although there may be slightly larger differences in the lower size ranges (<10–15 cm), the lines quickly converge. Despite the lack of significant change in the self-thinning line, biologically relevant growth components exhibited significant differences after 1990 (Fig. 8). Notably, there were higher mortality rates after 1990, but the maximum mortality decreased with increasing latitude. The pattern of mortality with age also changed, becoming flatter with increasing latitude. Additionally, the total biomass was higher and showed a significant increase after 1990, with the maximum total biomass decreasing with increasing latitude.

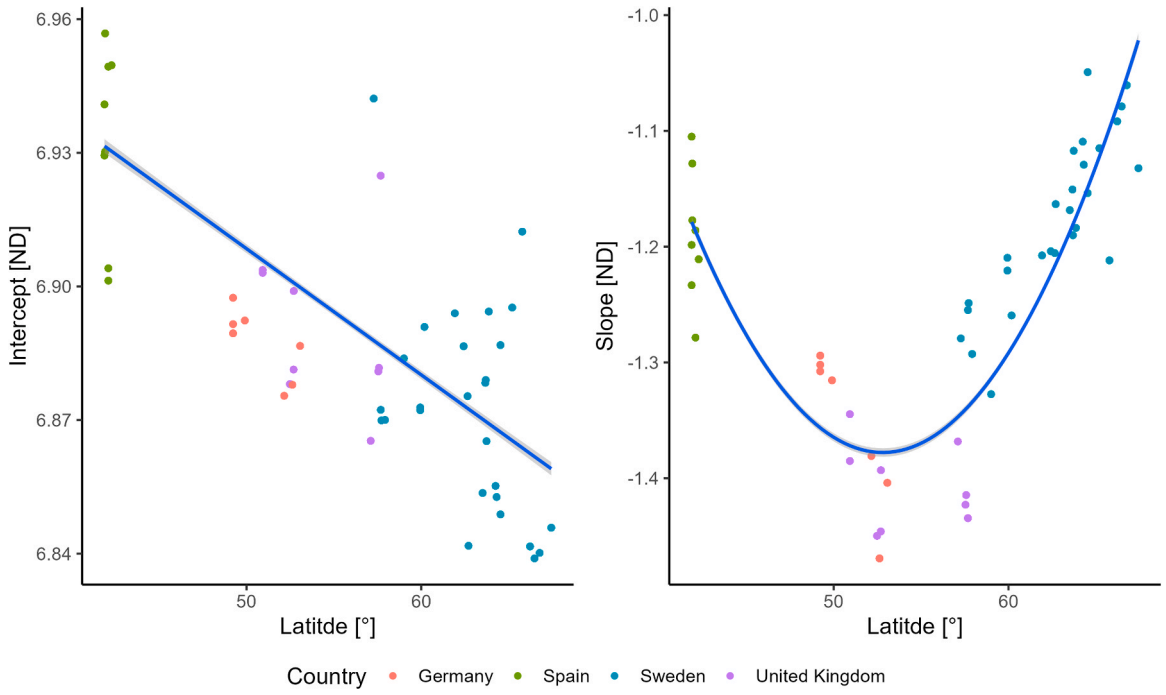

Fig. 6. Modelled intercepts (left) and slopes (right) from Fig. 5 against latitude, color-coded by country. On the left a line ($y = a + bx$), and on the right a polynomial ($y = a + bx + cx^2$) was fitted to the intercepts and slopes, respectively. The standard error is represented by the grey bands.

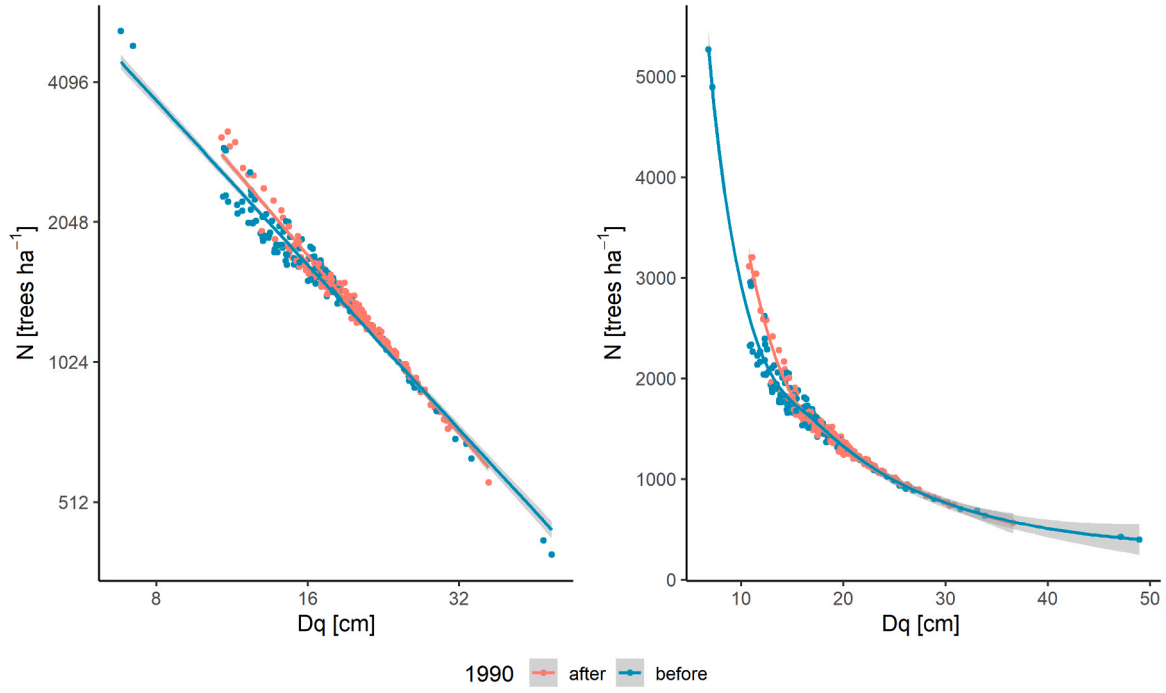

Fig. 7. Predicted self-thinning lines (Eq. 9) for the trial plots before (blue) and after (read) 1990, in linear double logarithmic form on the left and exponential on the right. The grey bands represent the standard error.

4. Discussion

4.1. Site patterns of self-thinning across Europe

The results of our analysis support the findings of earlier studies (Pretzsch and Biber, 2005; Weiskittel et al., 2009; Zhang et al., 2018) that have also shown that the self-thinning line is not constant (Q1). In our study, we further investigated the specific effects of site and climate parameters on the self-thinning line (Q2). We found that climate variables have different effects on the line, and we hypothesize that they can follow two species specific properties defined by Zeide (1985) between which trade-offs are common: the species' tolerance and self-tolerance. On the one hand, climate and site variables may increase species tolerance when increasing solar radiation which, in turn, flattens the slope. On the other hand, they can decrease self-tolerance, observed by a steepening of the slope caused by an increasing precipitation and

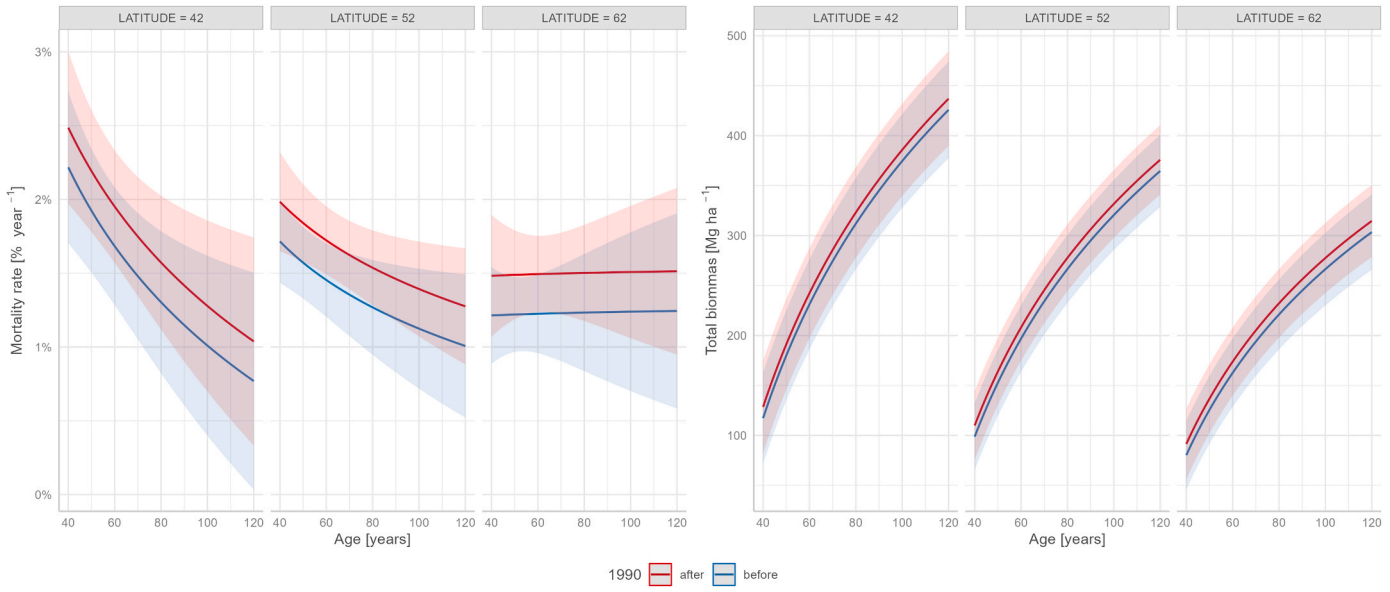

Fig. 8. Modeled changes in the mortality rate (left panel) and total biomass (right panel) for three latitudes in Europe before (blue) and after (red) 1990. Error bands are calculated with 95 % confidence interval.

temperature. This, in other words, means that intra-specific competition (self-tolerance) increases when precipitation and temperature are higher. These effects were particularly evident when analyzing the slope, showing the described counteracting effect (an increase in tolerance tends to decrease self-tolerance). However, the effects of climate variables on the intercept showed more variability and were more challenging to interpret, although a decrease with increasing latitudes was observed, which could be interpreted as a general decrease in productivity.

Similar self-thinning tendences have been observed in numerous works, but mainly showing results regarding temperature effects. In the case of Scots pine, Brunet-Navarro (2016) found similar tendencies for the temperature effect, with an increase in both the intercept and slope in hotter areas. Kimsey Jr. et al. (2019)) also observed an increase in maximum density with higher water supply for coniferous species, and Zahn et al. (2018) noted a steeper slope with higher precipitation for Chinese fir. However, the effects of temperature were different. Since Scots pine, like Chinese fir, is a shade-intolerant species, we could conclude that changes in solar radiation may have a stronger impact on crown architecture and therefore the self-tolerance of the species. This can be supported by the fact that the mean maximum temperature observed across the climatic gradient in Europe reported by Zhang et al. (2018) may be more closely connected to the temperature indicator estimated in our study, thus showing agreement with the negative effects we observed.

The range of slopes (–1.469 to –1.049) obtained from our model (Eq. 9) was closer to the estimates of Pretzsch and Biber (2005) and Weiskittel et al. (2009), but still less negative than the –1.605 reported by Reineke (1933) or later studies like del Río (2021). This can be explained by the fact that our stands may not be at maximum density and may encompass periods of self-thinning as well as periods without self-thinning, resulting in effective self-thinning occurring below the maximum density. Weiskittel et al. (2009) reported a slope range of –1.2 to –2.5 but did not identify the main drivers behind it. Zhang et al. (2018) also reported a broad range of –4.2 to –1.6, although they reported that values steeper than –2 may indicate flaws in the data. The influence of climate on the self-thinning slope is also consistent with the findings of Peters et al. (2018), who reported a dependence of the slope on water availability, with slope values ranging from –1.74 for humid areas to –0.95 for arid areas.

The inclusion of the Martonne Index in our analysis provided further support for our conclusions and helped explain the temperature effect on the self-thinning line. We observed that the Martonne Index steepens the line but increases the intercept. This finding is consistent with the study by Condés et al. (2017), which showed a similar tendency for the intercept but the opposite for the slope. This agreement with our data can be attributed to the fact that permanent plots are typically established in high-quality sites. The Martonne Index is an indicator of productivity, so for these high-quality sites where extreme water limitations are not expected, an increase in temperature leads to increased productivity and, consequently, enhanced competition, resulting in a decreasing effect of self-tolerance. Similarly, the site index has been identified as a key factor influencing the dynamics and self-thinning behavior of species such as Douglas fir, as it influences the allometric relationship between tree size and biomass (Weiskittel et al., 2009).

As previously mentioned, the observed differences among the countries in our study can primarily be attributed to changes in solar radiation, making it the main factor affecting changes in the self-thinning line. Therefore, we concluded that the sites analyzed in our study are characterized by a more light-limited rather than water-limited environment. Even the Spanish sites, located at high altitudes, exhibit temperatures and precipitation levels comparable to those within the typical distribution range of Scots pine. The higher effect of solar radiation in Spain compared to other countries suggests that changes in crown architecture or space demand may represent adaptations to higher solar radiation levels.

4.2. *Interpretation at tree level*

The U-shaped curve of slope against latitude (Fig. 6) has implications at the individual tree level. Crown expansion and growth adaptations influence the demand for growing space, which is inversely related to the maximum number of individuals (Pretzsch et al., 2012). Solar radiation, as a measure of light availability, plays a role in defining crown architecture and the bandwidth of allometric relationships (that is the potential allometric relationships for a certain species, depending on site parameters and the competition constellation) (Stenberg et al., 1994). Thus, our hypothesis suggests that changes in temperature and precipitation further affect the self-thinning line at the stand level by modifying a tree's ability to withstand competition.

In stands with high solar radiation, such as in Spain, we expect a higher tolerance to competition, and increase densities due to more

tolerance for multiple layers, but wider crown architectures that demand more space (Stenberg et al., 1994). However, when water and temperature are also high, the faster growth associated with these conditions translates into increased competition and a higher demand for growing space. These opposing effects tend to compensate for each other, particularly at the gradient's edges. In regions with sufficient solar radiation, but average precipitation and temperature (e.g., Germany and United Kingdom), the self-thinning slope reaches its maximum and is closest to the theoretical value proposed by Reineke (–1.605). Conversely, sites in Northern Sweden with low solar radiation may exhibit potentially longer crowns, but if accompanied by low temperature and precipitation, the slower productivity reduces the demand for growing space, resulting in narrower and denser crowns (Stenberg et al., 1994).

In conclusion, the U-shaped curve in the slope-latitude relationship has implications at both the individual tree and stand level. Light availability, temperature, and precipitation interact to influence crown architecture, self-tolerance, and the demand for growing space, ultimately shaping the self-thinning line. This understanding contributes to our knowledge of self-thinning dynamics across varying climatic conditions.

4.3. Temporal variation

The impact of time, specifically potential climate change, was also assessed (Q3). By examining the length of the vegetation period, we could identify changes in growing conditions before and after 1990. While mean solar radiation is not influenced by climate change, temperature and precipitation are, and they have the potential to modify the self-thinning line. However, no significant changes in the model were observed during this period.

The increase in temperature likely contributed to an increased rate of mortality along the self-thinning line, as evidenced by a significant rise in mortality after 1990 across Europe at all latitudes (Fig. 8, left). The model predicted a similar increase in mortality, with decreasing absolute levels as latitude increased, indicating that higher growth rates corresponded to higher mortality rates. The lengthening of the vegetation period is expected to symmetrically increase growth for all trees (Peters et al., 2018). Consequently, we interpret that the heightened growth resulting from the extended vegetation period accelerates mortality symmetrically for all trees, without altering the allometric relationships at the individual tree level.

The fact that no significant changes were found in the self-thinning line after 1990, suggests a faster self-thinning process due to accelerated mortality in unthinned stands over time. Currently, the impact of climate change appears to modify growth (Pretzsch et al., 2023) without affecting the allometry and tolerance of individual trees and stands, thus accelerating the self-thinning process proportionally to size. However, it is possible that the climate variables have not yet exhibited sufficient variation to induce changes in the allometry of Scots pine. Nevertheless, these effects vary across latitudes, showing flatter mortality trends in Northern latitudes, driven by lower productivity and symmetric mortality patterns (Pretzsch et al., 2022).

4.4. Implications for silviculture, modelling and climate change

The observation that the self-thinning line remained unchanged with time, while mortality rates varied, suggests the need for higher thinning frequencies, increased removal volumes, and shorter rotations in managed stands to take advantage of their accelerated growth (Pretzsch and Biber, 2021). However, it is important to adapt silvicultural guidance based on the self-thinning line to different latitudes. In mid-latitudes such as Germany and the UK, the data revealed the steepest slopes, closest to the estimates of Pretzsch and Biber (2005) and Reineke (1933). In these regions, the combination of relatively high average precipitation and temperature accelerates self-thinning, which is not overly attenuated by solar radiation. As solar radiation plays a role in defining species tolerance, the regulation of competition should be adjusted considering temperature and precipitation.

In growth models, it is crucial to adapt processes related to mortality and silvicultural regulation that rely on self-thinning (Ducey et al., 2017; Rodríguez de Prado et al., 2020) to different latitudes and account for the acceleration induced by climate changes. This adaptation would have the potential to enhance the accuracy of simulations and improve the ability to effectively manage forests.

4.5. Permanent plots of Scots pine

The unique collection of long-term experiments across Europe used in this study offers a comprehensive coverage of the geographical distribution of Scots pine, one of the most widely distributed tree species in Europe and highly valuable for silviculture and timber production (Kozakiewicz et al., 2020). The sites located at the edge of the natural distribution range, such as the Spanish sites, exhibit distinct characteristics in solar radiation compared to other sites. This highlights the importance of solar radiation in differentiating the characteristics of the self-thinning line across European regions. Additionally, when considering precipitation and temperature, the range of values observed in Spain is comparable to that of other countries, so we can conclude that solar radiation is main driving factor that distinguish the Spanish sites from the rest. Including data from countries like France or Italy would likely help fill the gaps in the described gradient.

The value of using permanent plots lies in the utilization of reliable data collected without management interventions, ensuring self-thinning conditions (though not necessarily maximum density). Studies such as Weiskittel et al. (2009) and Zeide (1985) have highlighted the advantages of permanent plots over inventory points, as the latter may not always reflect the maximum size-density relationship due to genetic or environmental constraints. By using a large dataset, this study aimed to narrow the range of slopes and account for the effects of stands that exhibit self-thinning as well as those that deviate from it (Pretzsch et al., 2019). Furthermore, this approach avoids the need for methods like quantile regressions, which rely on the arbitrary selection of thresholds or quantiles (Zhang et al., 2005).

CRediT authorship contribution statement

Toraño Caicoya: Conceptualization, Data curation, Formal analysis, Investigation, Methodology, Software, Supervision, Visualization, Writing original draft, Writing review & edit. **Biber:** Conceptualization, Funding acquisition, Data curation, Methodology, Supervision, Visualization, Writing review & edit. **Del Río:** Data curation, Investigation, Writing review & edit. **Ruiz-Peinado::** Data curation, Writing review & edit, **Arcangeli:** Data curation, Writing review & edit. **Mathews:** Data curation. **Pretzsch:** Conceptualization, Funding acquisition, Project admin, Data curation, Methodology, Supervision, Visualization, Writing review & edit.

Declaration of Competing Interest

The authors declare that they have no known competing financial interests or personal relationships that could have appeared to influence the work reported in this paper.

Data Availability

Data will be made available on request.

Acknowledgements

This publication has received funding from the European Union's HORIZON 2020 research and innovation program under the Marie

Skłodowska-Curie grant agreement N°778322. All authors would like to acknowledge the involved institutions in the participating countries for sharing permanent experiment data and the tremendous effort of collecting the data. We would like to thank the Bayerische Staatsforsten (BaySF) and the Nordwestdeutsche Forstliche Versuchsanstalt (NW-FA) for providing experimental plots in Germany, to the different projects of Instituto de Ciencias Forestales (ICIFOR-INIA, CSIC) in Spain; the Forestry Commission's Science and Innovation Strategy and also to Forest Research Sample Plot Officers and Technical Service staff in Britain and the Swedish University of Agricultural Sciences, Alnarp and Asa, in Sweden.

Appendix A. Supporting information

Supplementary data associated with this article can be found in the online version at doi:10.1016/j.foreco.2023.121585.

References

Aguirre, A., del Río, M., Condés, S., 2018. Intra- and inter-specific variation of the maximum size-density relationship along an aridity gradient in Iberian pinewoods. For. Ecol. Manag. 411, 90–100. https://doi.org/10.1016/j.foreco.2018.01.017.

Akaike, H., 1974. A new look at the statistical model identification. IEEE Trans. Autom. Control 19, 716–723. https://doi.org/10.1109/TAC.1974.1100705.

Barr, D.J., Levy, R., Scheepers, C., Tily, H.J., 2013. Random effects structure for confirmatory hypothesis testing: keep it maximal. J. Mem. Lang. 68, 255–278. https://doi.org/10.1016/j.jml.2012.11.001.

Begon, M., Townsend, C.R., Harper, J.L., 2006. Ecology: From Individuals to Ecosystems, 4th ed. ed.,. Blackwell Pub,, Malden, MA.

Belay, T.A., Moe, S.R., 2012. Woody dominance in a semi-arid savanna rangeland – evidence for competitive self-thinning. Acta Oecol. 45, 98–105. https://doi.org/10.1016/j.actao.2012.10.006.

Bose, A.K., Weiskittel, A., Kuehne, C., Wagner, R.G., Turnblom, E., Burkhart, H.E., 2018. Does commercial thinning improve stand-level growth of the three most commercially important softwood forest types in North America? For. Ecol. Manag. 409, 683–693. https://doi.org/10.1016/j.foreco.2017.12.008.

Brunet-Navarro, P., Sterck, F.J., Vayreda, J., Martinez-Vilalta, J., Mohren, G.M.J., 2016. Self-thinning in four pine species: an evaluation of potential climate impacts. Ann. For. Sci. 73, 1025–1034. https://doi.org/10.1007/s13595-016-0585-y.

CGMS [WWW Document], 2014. URL ⟨https://data.europa.eu/euodp/en/data/dataset/jrc-marsop4–7-weather_obs_grid_2015⟩ (accessed 12.17.19).

Charru, M., Seynave, I., Morneau, F., Rivoire, M., Bontemps, J.-D., 2012. Significant differences and curvilinearity in the self-thinning relationships of 11 temperate tree species assessed from forest inventory data. Ann. For. Sci. 69, 195–205. https://doi.org/10.1007/s13595-011-0149-0.

Condés, S., Vallet, P., Bielak, K., et al., 2017. Climate influences on the maximum size-density relationship in Scots pine (Pinus sylvestris L.) and European beech (Fagus sylvatica L.) stands. For. Ecol. Manag. 385, 295–307. https://doi.org/10.1016/j.foreco.2016.10.059.

Ducey, M.J., Knapp, R.A., 2010. A stand density index for complex mixed species forests in the northeastern United States. Forest Ecology and Management 260, 1613–1622. https://doi.org/10.1016/j.foreco.2010.08.014.

Ducey, MJ., Woodall, CW., Bravo-Oviedo, A., 2017. Climate and species functional traits influence maximum live tree stocking in the Lake States, USA. Forest Ecology and Management 386, 51–61. https://doi.org/10.1016/j.foreco.2016.12.007.

Forrester, D.I., et al., 2017. Generalized biomass and leaf area allometric equations for European tree species incorporating stand structure, tree age and climate. For. Ecol. Manag. 396, 160–175.

Forrester, Baker, D.I., Elms, T.G., et al., 2021. Self-thinning tree mortality models that account for vertical stand structure, species mixing and climate. For. Ecol. Manag. 487, 118936 https://doi.org/10.1016/j.foreco.2021.118936.

Gadow, K., von, 1986. Observations on self-thinning in pine plantations. South Afr. J. Sci. 82, 364–368.

Gadow, K. von, 2006. Forsteinrichtung: adaptive Steuerung und Mehrpfadprinzip, Universitätsdrucke Göttingen. Univ.-Verl. Göttingen, Göttingen.

IPCC, WMO (Eds.), 1992. Climate change: the 1990 and 1992 IPCC assessments, IPCC first assessment report overview and policymaker summaries and 1992 IPPC supplement. IPCC, Geneve.

ISIMP, 2022. ISIMIP Data Search | ISIMIP | ESGF-CoG [WWW Document]. URL https://esg.pik-potsdam.de/search/isimip/ (accessed 2.16.22).

Jack, S.B., Long, J.N., 1996. Linkages between silviculture and ecology: an analysis of density management diagrams. For. Ecol. Manag. 86, 205–220.

Kimsey, M.J., Shaw, T.M., Coleman, M.D., 2019. Site sensitive maximum stand density index models for mixed conifer stands across the Inland Northwest, USA. For. Ecol. Manag. 433, 396–404. https://doi.org/10.1016/j.foreco.2018.11.013.

Kozakiewicz, P., Jankowska, A., Mamiński, M., Marciszewska, K., Ciurzycki, W., Tulik, M., 2020. The wood of Scots pine (Pinus sylvestris L.) from Post-agricultural Lands Has Suitable Properties For The Timber Industry. Forests 11, 1033. https://doi.org/10.3390/f11101033.

Lonsdale, W.M., Watkinson, A.R., 1982. Light and self-thinning. N. Phytol. 90, 431–445. https://doi.org/10.1111/j.1469-8137.1982.tb04476.x.

Martonne, E., de, 1926. L'indice d'aridité. Bull. De. l'Association De. Géographes Fr. 3, 3–5. https://doi.org/10.3406/bagf.1926.6321.

Peters, R., Olagoke, A., Berger, U., 2018. A new mechanistic theory of self-thinning: adaptive behaviour of plants explains the shape and slope of self-thinning trajectories. Ecol. Model. 390, 1–9. https://doi.org/10.1016/j.ecolmodel.2018.10.005.

Pretzsch, H., Biber, P., 2005. A re-evaluation of Reineke's rule and stand density index. For. Sci. 51, 304–320. https://doi.org/10.1093/forestscience/51.4.304.

Pretzsch, H., Biber, P., 2021. Fertilization modifies forest stand growth but not stand density: consequences for modelling stand dynamics in a changing climate. For.: Int. J. For. Res. https://doi.org/10.1093/forestry/cpab036 cpab036.

Pretzsch, H., Matthew, C., Dieler, J., 2012. Allometry of Tree Crown Structure. Relevance for Space Occupation at the Individual Plant Level and for Self-Thinning at the Stand Level, in: Matyssek, R., Schnyder, H., Oßwald, W., Ernst, D., Munch, J.C., Pretzsch, Hans (Eds.), Growth and Defence in Plants: Resource Allocation at Multiple Scales, Ecological Studies. Springer, Berlin, Heidelberg, pp. 287–310. https://doi.org/10.1007/978–3-642–30645-7_13.

Pretzsch, H., Biber, P., Schütze, G., Uhl, E., Rötzer, T., 2014. Forest stand growth dynamics in Central Europe have accelerated since 1870. Nat. Commun. 5, 4967 https://doi.org/10.1038/ncomms5967.

Pretzsch, H., Biber, P., Uhl, E., Dahlhausen, J., Schütze, G., Perkins, D., Rötzer, T., Caldentey, J., Koike, T., Con, T. van, Chavanne, A., Toit, B. du, Foster, K., Lefer, B., 2017. Climate change accelerates growth of urban trees in metropolises worldwide. Sci. Rep. 7, 15403 https://doi.org/10.1038/s41598-017-14831-w.

Pretzsch, H., del Río, M., Biber, P., et al., 2019. Maintenance of long-term experiments for unique insights into forest growth dynamics and trends: review and perspectives. Eur. J. For. Res. 138, 165–185. https://doi.org/10.1007/s10342-018-1151-y.

Pretzsch, H., Bravo-Oviedo, A., Hilmers, T., et al., 2022. With increasing site quality asymmetric competition and mortality reduces Scots pine (Pinus sylvestris L.) stand structuring across Europe. For. Ecol. Manag. 520, 120365 https://doi.org/10.1016/j.foreco.2022.120365.

Pretzsch, H., del Río, M., Arcangeli, C., Bielak, K., Dudzinska, M., Forrester, D.I., Klädtke, J., Kohnle, U., Ledermann, T., Matthews, R., Nagel, J., Nagel, R., Ningre, F., Nord-Larsen, T., Biber, P., 2023. Forest growth in Europe shows diverging large regional trends. Sci. Rep. 13, 15373 https://doi.org/10.1038/s41598-023-41077-6.

Reineke, L.H., 1933. Perfecting a stand-density index for even-aged forests. J. Agric. Res. 46, 627–638.

Reynolds, J.H., Ford, E.D., 2005. Improving competition representation in theoretical models of self-thinning: a critical review. J. Ecol. 93, 362–372. https://doi.org/10.1111/j.1365-2745.2005.00976.x.

del Río, M., Montero, G., Bravo, F., 2001. Analysis of diameter–density relationships and self-thinning in non-thinned even-aged Scots pine stands. For. Ecol. Manag. 142, 79–87. https://doi.org/10.1016/S0378-1127(00)00341-8.

Rodríguez de Prado, D., San Martín, R., Bravo, F., Herrero de Aza, C., 2020. Potential climatic influence on maximum stand carrying capacity for 15 Mediterranean coniferous and broadleaf species. For. Ecol. Manag. 460, 117824 https://doi.org/10.1016/j.foreco.2019.117824.

Stenberg, P., Kuuluvainen, T., Kellomäki, S., Grace, J.C., Jokela, E.J., Gholz, H.L., 1994. Crown structure, light interception and productivity of pine trees and stands. Ecol. Bull. 20–34.

Weiskittel, A., Gould, P., Temesgen, H., 2009. Sources of variation in the self-thinning boundary line for three species with varying levels of shade tolerance. For. Sci. 55, 84–93. https://doi.org/10.1093/forestscience/55.1.84.

Woodall, C.W., Weiskittel, A.R., 2021. Relative density of United States forests has shifted to higher levels over last two decades with important implications for future dynamics. Sci. Rep. 11, 18848 https://doi.org/10.1038/s41598-021-98244-w.

Zeide, B., 1985. Tolerance and self-tolerance of trees. For. Ecol. Manag. 13, 149–166. https://doi.org/10.1016/0378-1127(85)90031-3.

Zeide, B., 2010. Comparison of self-thinning models: an exercise in reasoning. Trees 24, 1117–1126. https://doi.org/10.1007/s00468-010-0484-z.

Zhang, L., Bi, H., Gove, J.H., Heath, L.S., 2005. A comparison of alternative methods for estimating the self-thinning boundary line. Can. J. For. Res. 35, 1507–1514. https://doi.org/10.1139/x05-070.

Zhang, X., Lu, L., Cao, Q.V., Duan, A., Zhang, J., 2018. Climate-sensitive self-thinning trajectories of Chinese fir plantations in south China. Can. J. For. Res. https://doi.org/10.1139/cjfr-2018-0168.